Anal. Bioanal. Electrochem., Vol. 8, No. 8, 2016, 1012-1032

Analytical & Bioanalytical Electrochemistry

2016 by CEE
www.abechem.com

Full Paper

Corrosion Inhibition and Adsorption Behavior of 5-(phenylthio)-3H-pyrrole-4-carbonitriles on Mild Steel Surface in 1M H_2SO_4: Experimental and Computational Approach

Chandrabhan Verma, M. A. Quraishi* and Rishi Korde

Department of Chemistry, Indian Institute of Technology, Banaras Hindu University, Varanasi 221005, India

*Corresponding Author, Tel.: +91-9307025126; Fax: +91- 542- 2368428
E-Mail: maquraishi.apc@itbhu.ac.in; maquraishi@rediffmail.com

Received: 7 September 2016 / Received in revised form: 5 November 2016 / Accepted: 18 November 2016 / Published online: 31 December 2016

Abstract- Present study describes the effect of electron donating hydroxyl (-OH) group (s) on adsorption behavior of three 5-(phenylthio)-3H-pyrrole-4-carbonitriles (PPCs) on mild steel corrosion in 1 M H_2SO_4 using gravimetric, Tafel polarization and impedance spectroscopy (EIS), quantum chemical calculations and molecular dynamics simulations methods. The inhibitors showed the maximum efficiency of 91.32%, 92.97% and 94.62% for PPC-I, PPC-II and PPC-III, respectively at 1.29×10^{-4} mol/L concentration and behaved as mixed type inhibitors. Adsorption of studied inhibitors on mild steel surface followed the Langmuir adsorption isotherm. The quantum chemical calculation parameters such as E_{HOMO}, E_{LUMO}, ΔE, global harness, softness, electronegativity and fraction of electron transfer (DN) were calculated using DFT method to correlate the electronic properties with the adsorption behavior of studied molecules. The adsorption behavior of the inhibitor molecules was further supported by their adsorption energies using molecular dynamics simulations method.

Keywords - Adsorption, EIS/ Tafel, Quantum chemical calculations and molecular dynamics simulations

1. INTRODUCTION

Iron and its alloys are widely used in the several industries due to their low cost and high mechanical strength [1]. However, they severally undergo corrosion during industrial

processes such as acid cleaning, acid descaling, acid acidization, acid pickling etc. [2]. To minimize metal dissolution in acid solution inhibitors are used. These inhibitors are adsorbed on metal, surface and inhibit corrosion [3]. The adsorption of these compounds on the metallic surface is influenced by several factors such as nature and charge on the metallic surface, nature of electron donating and electron withdrawing substituent of inhibitor, solution temperature, and nature of electrolyte [3]. Recently, computational techniques such as quantum chemical calculations and molecular dynamics simulations have immersed as tools for designing effective corrosion inhibitors and predicting their chemical reactivity [4]. Moreover, the quantum chemical calculations and molecular dynamics simulations methods have attracted great deal of interest for predicting adsorption behavior of inhibitor molecules even without synthesizing them [5]. Review of the literature reveals that nitrogen containing compounds act as efficient corrosion inhibitors in hydrochloric acid solution, while sulfur containing compounds act as good corrosion inhibitors in sulphuric acid solution [6,7]. And, compounds containing both nitrogen and sulfur acts as good inhibitors in hydrochloric as well as sulphuric acid solutions [6-8].

In view of the above observation, in our present investigation we report here the inhibition efficiency of three synthesized 5-(phenylthio)-3H-pyrrole-4-carbonitriles (PPCs) on mild steel corrosion in 1 M H_2SO_4 using weight loss, electrochemical, quantum chemical calculations and molecular dynamics simulations methods. The selection of 5-(phenylthio)-3H-pyrrole-4-carbonitriles (PPCs) as corrosion inhibitors in present study is based on the fact that these compounds possess several heteroatoms (S, N, and O) and polar functional groups (-OH, -NH_2, and -CN) and conjugated pi-electrons through which they can adsorb effectively over the metallic surface. Moreover, presence of several heteroatoms and polar functional groups likely enhance to the solubility of these compounds in the test solution. To the best of our knowledge this is the first time these compounds are being tested as inhibitors of mild steel corrosion in 1 M H_2SO_4. It is important to mention that the convenient synthesis of these compounds is reported by Das and co-workers [9] and inhibition properties of these compounds have been reported by Verma and coworkers [10] on mild steel corrosion in 1 M hydrochloric acid solution, however, their corrosion inhibition potentials for mild steel in 1 M H_2SO_4 medium have not been investigated. The inhibition performance of the studied molecules is also investigated using molecular dynamics simulation and electrostatic potential methods, in addition to the techniques used in our earlier measurement [10].

2. EXPERIMENTAL SECTIONS

Inhibitors used in the present study were synthesized by one step multi component coupling reaction of acetophenone derivatives, malononitrile and thiophenol in presence of triethyl amine as catalyst and water as solvent as described earlier [9] as shown in Fig. 1. The characterization data, IUPAC name and chemical structure of the undertaken inhibitor

molecules in the present study are given in Table 1. For weight loss, electrochemical and surface studies, the test material was mild steel. Chemical composition of the steel and method of sample preparation was same as described in earlier reports [1,3,10].

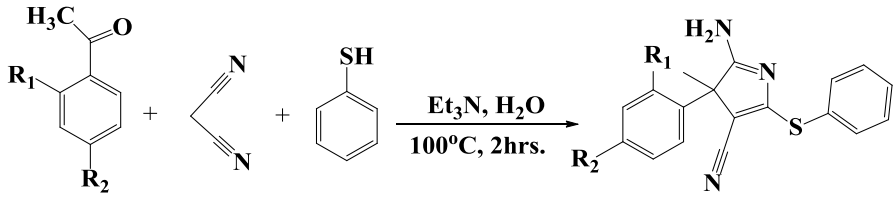

PPC-I:R_1=R_2= -H; PPC-II: R_1=-H, R_2=-OH; PPC-III: R_1= R_2 =-OH

Fig. 1. Synthetic route of the studied PPCs

The 100 ml solution of 1 M H_2SO4 was used for all weight loss and electrochemical measurements.

Table 1. IUPAC name, molecular structure, molecular formula, melting point and analytical data of the studied PPCs

S.No.	IUPAC name	Chemical structure	Molecular formula and M.P. and analytical data
1	2-amino-3-methyl-3-phenyl-5 -(phenylthio)-3H-pyrrole-4-carbonitrile **(PPC-I)**	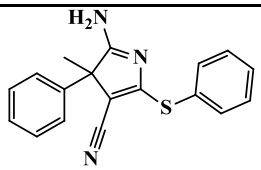	$C_{18}H_{15}N_3S$ (mol. wt. 305.39); Brown colored solid; MP: 208-209 ^{0}C, IR(KBr, 1/cm): 3484, 3436, 3345-3258, 3122, 2254, 1623, 1572-1521, 1452, 1163, 627; ^{1}H NMR (300 MHz, DMSO, δ, ppm, Me_4Si): 1.54, 6.99-7.10, 7.16-7.22, 7.29-7.49, 7.83, 7.92
2	2-amino-3-(4-hydroxyphenyl)-3-methyl-5-(phenylthio)-3H-pyrrole-4-carbonitrile **(PPC-II)**	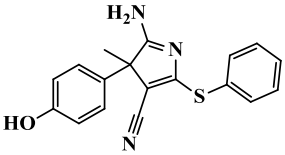	$C_{18}H_{15}N_3OS$ (mol. wt. 321.39); Cream colored solid; MP: 161-163 ^{0}C, IR(KBr, 1/cm): 3668, 3423, 3472-3318, 3185 (C-H), 2856, 2212, 1608-1563, 1483-1428, 1142, 622 ^{1}H NMR (300 MHz, DMSO, δ, ppm, Me_4Si): 1.62, 7.23-7.34, 7.45-7.56, 7.64-7.69, 7.98, 8.11
3	2-amino-3-(2,4-dihydroxyphenyl) -3-methyl-5-(phenylthio)-3H-pyrrole-4-carbonitrile **(PPC-III)**	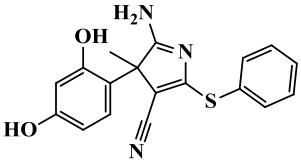	$C_{18}H_{15}N_3O_2S$ (mol. wt. 337.08); White colored solid; MP: 161-163 ^{0}C, IR(KBr, 1/cm): 3684-3673, 3446-3483, 3272, 2864, 2278, 1624-1596, 1511-1444, 1187 , 682 ^{1}H NMR (300 MHz, DMSO, δ, ppm, Me_4Si): 1.73, 7.31-7.39, 7.48-7.58, 7.69-7.72, 8.21-8.53

2.1. Weight loss experiments

The weight loss experiments were carried out using mild steel having exposed area of 10 cm^2 as exactly described previously our research group [1,3]. The inhibition efficiency (η%) was calculated from the average weight loss values using expression [1,3]:

$$\eta\% = \frac{w_o - w_i}{w_o} \times 100 \quad (1)$$

Where w_0 and w_i are the weight loss values without and with optimum concentrations of PPCs (the inhibitors), respectively.

2.2. Electrochemical experiments

The electrochemical experiments were performed on Gamry fitted with three electrode glass assembly as described previously. The potential of working electrode was allowed to varies inevitably from -0.25 to +0.25 V *vs*. corrosion potential (E_{corr}) at sweep rate of 1.0 mV s^{-1}. The extrapolation of cathodic and anodic curves furnishes the value of corrosion current (i_{corr}) in the absence and presence of investigated inhibitor molecules. The value of the percentage inhibition efficiency was calculated by the following equation [1,3]:

$$\eta\% = \frac{i^0_{corr} - i^i_{corr}}{i^0_{corr}} \times 100 \quad (2)$$

Where $i°_{corr}$ and i^i_{corr} are corrosion current in the absence and presence of studied inhibitor molecules PPCs, respectively.

An AC signal of 10 mV peak-to-peak amplitude was applied for EIS studies at the OCP in the frequency range of 100 kHz to 0.01 Hz. On fitting EIS data into the suitable circuit, the values of charge transfer resistances (R_{ct}) were derived from which the inhibition efficiency was derived as follows [1,3]:

$$\eta\% = \frac{R^i_{ct} - R^0_{cT}}{R^i_{ct}} \times 100 \quad (3)$$

Where, R_{ct}^{0} and R_{ct}^{i} are charge transfer resistances in the absence and presence of optimum concentrations of PPCs, respectively.

2.3. Scanning electron microscopy (SEM) analysis

The mild steel specimens were immersed in 1 M sulphuric acid for 3 hrs in the absence and presence of optimum concentration of PPC-III (best inhibitor) for scanning electron microscopic measurement. After elapsed time, specimens were taken out, washed with distilled water, degreased with acetone, dried under hot air blower and stored in moisture free desiccators before examining their surface. The surface morphologies of inhibited and

uninhibited metallic specimens were examined at 500x magnification using SEM model Ziess Evo 50 XVP modal.

2.4. Quantum chemical calculations study

The gradient correlation function as given by Lee, Yang and Parr (LYP) [7] was employed for all quantum chemical calculations in the present study. It is consists of the B3LYP, a version of the DFT method that uses Becke's three parameter functional (B3) and includes a combination of HF with DFT exchange terms. The geometry optimization of all investigated inhibitors at the B3LYP/6-31G (d) level were carried out using Gaussian'03 program package [11]. The value of chemical potential (ρ) can be considered as negative of the electronegativity (χ). The value of electronegativity (χ) for a system consisting of N-electrons with total electronic energy (E) an external potential (v (r)); can be calculated using following equation: [12]:

$$\chi = -\rho = -\left(\frac{\partial E}{\partial N}\right)_{v(r)} \tag{4}$$

The value of Hardness (η) is another DFT based parameter which describes the dependency of total electronic energy (E) on the N at v(r) property which in turn provides measurement of not only the stability of the molecules but also informs about the chemical reactivity the molecule. The value of Hardness (η) was calculated by employing by following relationship [1,3]:

$$\eta = \left(\frac{\partial^2 E}{\partial N^2}\right)_{v(\mathrm{r})} = \left(\frac{\partial \rho}{\partial N}\right)_{v(\mathrm{r})} \tag{5}$$

The fraction of transferred electrons (ΔN) from the PPCs molecules to the mild steel surface was evaluated using the calculated values of electronegativity (χ) and hardness (η) as follows [1,3]:

$$\Delta N = \frac{\chi_{Fe} - \chi_{inh}}{\left[2\left(\eta_{Fe} + \eta_{inh}\right)\right]} \tag{6}$$

Where, χ_{Fe} and χ_{inh} denote the iron and inhibitors absolute electronegativity, respectively; η_{Fe} and η_{inh} represent the absolute hardness of iron and the inhibitor molecules, respectively. It is previously reported that the value of ionization potential (I) corresponds E_{HOMO} and electron affinity (A) is corresponds to E_{LUMO} as given bellows [1,3]:

$$I = -E_{HOMO} \tag{7}$$

$$A = -E_{LUMO} \tag{8}$$

The value nucleophilic index (ω) which has been introduced as a new global chemical reactivity parameter, depend upon the chemical potential in addition to the global hardness by the following relation [1,3]:

$$\omega = \frac{\rho^2}{2\eta} \tag{9}$$

The value of global softness which is measure of degree of polarization and inversely related to value of global hardness can be calculated using following relation [1,3]:

$$\sigma = \frac{1}{\eta} \tag{10}$$

2.5. Molecular dynamics studies

The molecular dynamics simulations study on investigated inhibitors was performed using Material Studio 7.0 software which is commercially available software licensed Accelrys Inc. USA as described earlier by several authors [13].

3. RESULTS AND DISCUSSIONS

3.1. Weight loss experiments

3.1.1. Effect of inhibitors concentrations and solution temperatures

Table 2 shows the change in the percentage inhibition performance of the studied inhibitor molecules with respect to their concentrations.

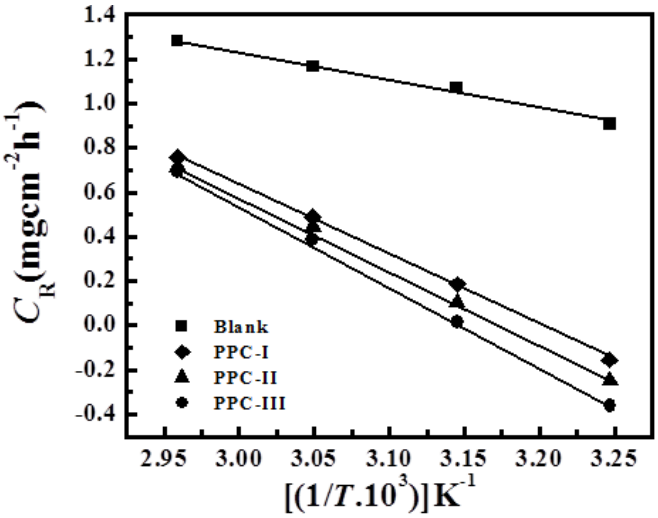

Fig. 2. Arrhenius plots for the corrosion of mild steel in 1 M H_2SO_4

Inspection of the depicted results showed that inhibition efficiencies of all studied inhibitors increases with increasing their concentrations and maximum value of inhibition efficiency were obtained at 1.29×10^{-4} mol/L concentration. The inhibition efficiencies of the studied compounds followed the order: PPC-III (91.32%) > PPC-II (92.97) > PPC-I (94.62%).

The higher inhibition efficiency of PPC-II as compare to PPC-I is attributed due to presence of electron releasing hydroxyl (-OH) group which increases the strength of adsorption due to its *+R* effect in form of two lone pairs of electrons on the oxygen atom. The highest inhibition efficiency of the PPC-III among the studied compounds could be as a result of stronger interaction between metal and inhibitor because PPC-III has one addition electron releasing hydroxyl group [1,14]. This decrease in the inhibition efficiency (Table 3) with increase in the temperature could be as a result of decrease in the interaction between inhibitors and metallic surface at elevated temperature due to increase in the kinetic energy of the inhibitor molecules [1,14].

Table 2. The weight loss parameters obtained for mild steel in 1 M H_2SO_4 containing different concentrations of PPCs

Inhibitor	Conc mol/L	Weight loss (mg)	C_R mgcm^{-2}h^{-1}	η%	θ
Blank	---	242	8.06	--	--
PPC-I	7.42×10^{-5}	88	2.93	63.63	0.6363
	1.48×10^{-4}	44	1.46	81.84	0.8181
	1.22×10^{-4}	33	1.10	86.36	0.8636
	1.29×10^{-4}	21	0.70	91.32	0.9132
PPC-II	7.42×10^{-5}	84	2.80	65.28	0.6528
	1.48×10^{-4}	39	1.30	83.88	0.8388
	1.22×10^{-4}	25	0.83	89.66	0.8966
	1.29×10^{-4}	17	0.56	92.97	0.9297
PPC-III	7.42×10^{-5}	78	2.60	67.76	0.6776
	1.48×10^{-4}	36	1.20	85.12	0.8515
	1.22×10^{-4}	21	0.70	91.32	0.9132
	1.29×10^{-4}	13	0.43	94.62	0.9462

The effect of temperature on the inhibition efficiency can be represented by Arrhenius equation [1,14]:

$$\log(C_R) = \frac{-E_a}{2.303RT} + \log A \qquad (11)$$

Where C_R is the corrosion rate in mgcm^{-2} h^{-1}, A is the Arrhenius pre-exponential factor, R is the gas constant and T is absolute temperature.

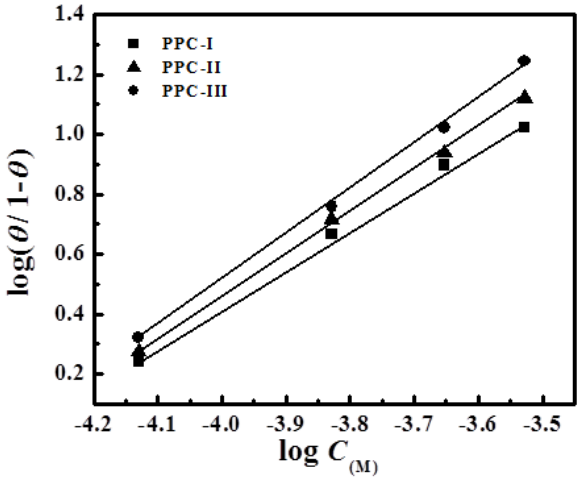

Fig. 3. Langmuir adsorption isotherm plots for the adsorption of PPCs on mild steel surface in 1 M H_2SO_4

The values of intercept, slopes, regression coefficient (R^2) and activation energies (E_a) calculated from the Arrhenius plots (Fig. 2) are given in Table 4. The higher values of E_a in presence of inhibitor molecules as compare to in their absence (24.28 kJ mol^{-1}) suggest that in presence of inhibitors corrosion become more difficult owing to the formation protective surface of inhibitor molecules on the steel surface that separates the metal corrosive acid solution [15].

3.1.2. Adsorption isotherms

The mechanism and strength of adsorption cab be provided by adsorption isotherm and therefore, adsorption isotherm is very most important topic in the field of corrosion study. It also provides some thermodynamic information's along with few vital parameters such as Gibb's free energy (ΔG^0_{ads}) and adsorption constant (K_{ads}).

Table 3. Variation of C_R and η % with temperature in the absence and presence of optimum concentration of PPCs in 1 M H_2SO_4

Temperature (K)	Corrosion rate (CR) and inhibition efficiency (η%)							
	Blank		**PPC-I**		**PPC-II**		**PPC-III**	
	C_R	η%	C_R	η%	C_R	η%	C_R	η%
308	8.06	--	0.70	91.32	0.56	92.97	0.43	94.62
318	11.73	--	1.53	86.93	1.26	89.20	1.03	91.19
328	14.60	--	3.06	78.99	2.80	80.82	2.43	83.33
338	19.06	--	5.73	69.93	5.20	72.72	4.93	74.12

In our present study the Langmuir isotherm gave the best fit with values of regression coefficient (R^2) close to one. The Langmuir isotherm can be best represented by following relationship [14]:

$$K_{ads}C = \frac{\theta}{1-\theta} \quad (12)$$

In the above equation, K_{ads} represents the equilibrium constant for the adsorption and desorption of inhibitor molecules, C is the inhibitor concentration and θ is the surface coverage. The intercept of the straight lines of the Langmuir isotherm plots (Fig. 3) furnished the values of K_{ads} for all inhibitors at different studied temperature which are given in the Table 5.

Table 4. Values of intercepts, slopes, regression coefficients (R^2) and activation energies for mild steel dissolution in 1 M H_2SO_4 in the absence and presence of optimum concentration of PPCs

Inhibitor	**Intercept**	**slope**	**(R^2)**	***E_a***
Blank	-1.2684	5.0372	0.9941	24.28
PPC-I	-3.1697	10.145	0.9995	60.69
PPC-II	-3.3698	10.701	0.9988	64.52
PPC-III	-3.6902	11.622	0.9994	70.66

The values of Gibb's free energy (ΔG^0_{ads}) was calculated by employing the obtained values of the K_{ads} according to the following equation:

$$\Delta G^0_{ads} = -RT \ln (55.5\, K_{ads}) \quad (13)$$

Table 5. The values of K_{ads} and ΔG°_{ads} for mild steel in 1 M H_2SO_4 in the absence and presence of optimum concentration of PPCs at different temperatures

Inhibitor	**K_{ads} (10^4 M^{-1})**				**$-\Delta G^\circ_{ads}$ (k $Jmol^{-1}$)**			
	308	318	328	338	308	318	328	338
PPC-I	1.26	0.79	0.45	0.27	34.47	34.38	33.91	33.59
PPC-II	1.5	0.99	0.50	0.32	35.06	34.95	34.22	33.97
PPC-III	2.11	1.24	0.60	0.34	35.79	35.54	34.68	34.17

Where, numeric value 55.5 represents the molar concentration of water in the acid solution. The calculated values of ΔG^0_{ads} are given Table 5. The negative sign of the ΔG^0_{ads} suggest the spontaneous nature of adsorption of inhibitor molecules on the mild steel surface [1,14]. The lower values of ΔG^0_{ads} than -40 kJmol^{-1} for investigated inhibitor molecules suggest that the adsorption of studied compounds on metal surface involves physisorption [15,16].

3.2. Electrochemical studies

3.2.1. Open circuit potential (OCP) analysis

The effect of optimum concentration of PPCs on the open circuit potential of mild steel corrosion in 1 M H_2SO_4 is depicted in Fig. 4. Examination of the Fig. 4 reveals that OCP curves are similar for inhibited and uninhibited mild steel specimens suggesting that presence of inhibitors did not change the mechanism of corrosion. Moreover, it is seen that OCP shifted toward highly negative direction indicating the dissolution of oxide layer formed over the metallic surface [17,18]. Additionally, in presence of PPCs OCP shifted towards more noble direction which is attributed due to further breakdown of oxide layer and formation of protective film by the inhibitor molecules over the mild steel surface [17-20].

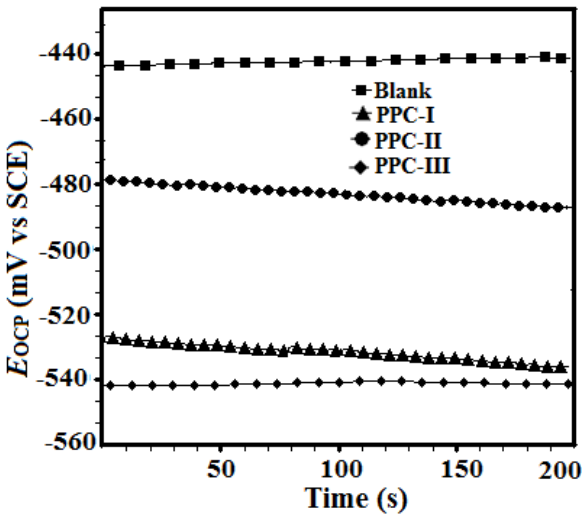

Fig. 4. The effect of PPCs on the open-circuit potential of mild steel in 1 M H_2SO_4

3.2.2. Tafel polarization studies

The Tafel polarization curves of the mild steel in 1 M H_2SO_4 solution at optimum concentration of the studied inhibitors are given in Fig. 4.

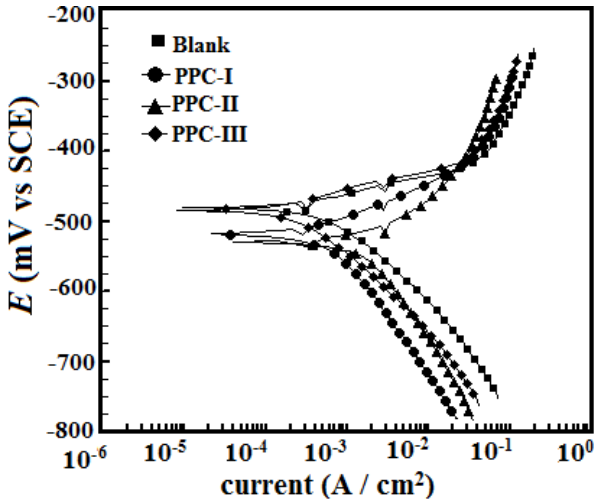

Fig. 5. Tafel polarization curves for mild in the absence and presence of optimum concentration of PPCs

The Tafel polarization is presented in Table 6. It can be seen from the results (Fig. 4 and Table 6) that both cathodic and anodic reactions were affected by the inhibitor molecules with maximum displacement of 56mV in the value of E_{corr} suggesting that all studied inhibitors acts as mixed type inhibitors. However, careful examination of the Table 6 showed that variation in the values of β_c are more prominent as compare to the value of β_a suggesting that the inhibitor molecules acted as cathodic type inhibitors, in spite of the fact that the maximum change in the value of E_{corr} is less than -85mV [21].

Table 6. Tafel polarization parameters for mild steel in 1M H_2SO_4 solution in the absence and presence of optimum concentrations of PPCs

Inhibitor	**Conc** mol/L	E_{corr} (mV/SCE)	β_a (μA/cm^2)	β_c (mV/dec)	i_{corr} (mV/dec)	η%	θ
Blank	---	-476	83.10	228.8	2010	----	----
PPC-I	1.29×10^{-4}	-478	74.7	124.7	180.0	91.04	0.9104
PPC-II	1.29×10^{-4}	-529	89.9	93.8	148.0	92.63	0.9263
PPC-III	1.29×10^{-4}	-532	81.5	69.3	95.0	95.27	0.9527

3.2.3. Electrochemical impedance spectroscopic (EIS) studies

Nyquist plots and the corresponding Bode plots for mild steel dissolution in 1 M H_2SO_4 solution in presence of optimum concentration of the PPCs are shown in Fig. 5a and b, respectively. From Fig. 5 it can be seen that Nyquist plots show depressed semicircle with one time constant in Bode plots in the absence and presence of optimum concentration of the

inhibitor molecules which is an indication that corrosion of mild steel in 1M H_2SO_4 is mainly controlled by charge transfer reaction [14,21]. In our present case, the capacitance was replaced by constant phase element (CPE) because it gives better approximation. CPE is defined in impedance representation as [22]:

$$Z_{\mathrm{CPE}} = \left(\frac{1}{Y_0}\right)[(j\omega)_n]^{-1} \tag{14}$$

Where, Y_0 is the CPE constant, j is the imaginary number, ω is the angular frequency, and n is the phase shift (exponent) which is measure of the surface inhomogeneity.

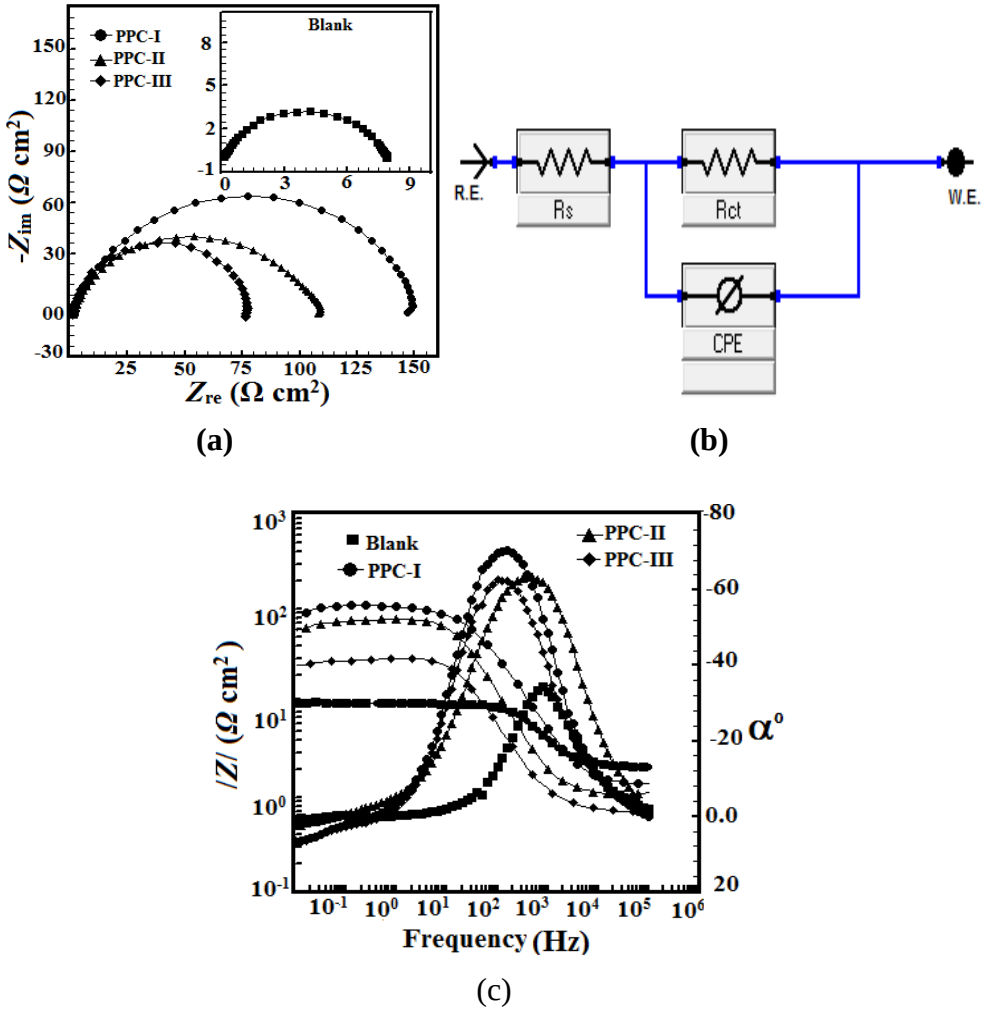

Fig. 5. (a) Nyquist plot for mild steel in 1 M H_2SO_4 in the absence and presence of optimum of concentrations of PPCs; (b) Equivalent circuit used for the analysis of the EIS spectra; (c) Bode plots for mild steel in 1 M H_2SO_4 in the absence and presence of optimum of concentrations of PPCs

Generally, a lower value of n associated with high degree of surface inhomogeneity and vice versa. Further, depending on the value of n, CPE can represents the resistance (n=0),

capacitance (n=1) or inductance (n=1) nature of the electric double layer. The values double layer capacitance (C_{dl}) in the absence and presence of inhibitors was derived as [14,23]:

$$C_{dl}=Y_0\ (\omega max)^{n-1} \quad (15)$$

Where, ω_{max} represents the frequency at the point of which the imaginary part of impedance has gained the maximum (rad s^{-1}) value.

Table 7. EIS parameters obtained for mild steel in 1M H_2SO_4 in the absence and presence of optimum concentrations of PPCs

Inhibitor	**Conc** mol/L	R_s (Ω cm^2)	R_{ct} (Ω cm^2)	n	Y_0 (μF cm^{-2})	C_{dl} (μF cm^{-2})	η%	θ
Blank	---	0.89	6.95	0.858	183.00	75.18	----	----
PPC-I	1.29×10^{-4}	1.10	76.53	0.935	84.00	55.55	91.31	0.9131
PPC-II	1.29×10^{-4}	0.85	117.94	0.964	62.50	50.89	94.10	0.9410
PPC-III	1.29×10^{-4}	1.01	151.29	0.986	43.00	39.49	95.40	0.9540

The common electrochemical impedance parameters calculated with the help of equivalent circuit shown in Fig. 5c and are given in Table 7. Form the results shown in Table 7 it can be observed that values of R_{ct} for inhibited solution are much higher as compare to uninhibited solution which clearly suggests that investigated compounds inhibit mild steel corrosion in the testing medium by forming protective surface film through adsorption which reduces the active surface area of the adsorbing on the mild steel surface [23,24]. It is evident from the Table 7 that values of C_{dl} have decreased in presence of the studied inhibitor molecules which attributed due to their adsorption at metal/ solution interface and increased thickness of the electric double layer [23,24].

3.3. Scanning electron microscopic (SEM) analysis

Fig. 6 represents the SEM micrographs of inhibited and uninhibited mild steel specimens. Careful inspection shows that mild steel surface in the absence of inhibitors (Fig.6a) is highly corroded and damaged due to free acid attack. However, surface morphology of the inhibited mild steel specimen by PPC-III shows remarkable smoothness in the surface morphology. The metallic specimen is less corroded and damaged indicating that in the presence of inhibitor dissolution of metal is inhibited which is attributed due to formation of protective covering over the metallic surface.

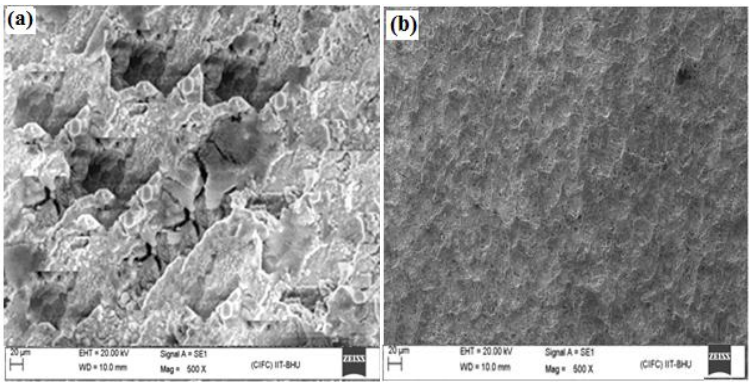

Fig. 6. Scanning electron microscopic micrographs of uninhibited (a), and inhibited (b) mild Steel specimens

3.4. Quantum chemical calculations

The fully optimized structures of the studied inhibitor molecules are shown in Fig. 6.

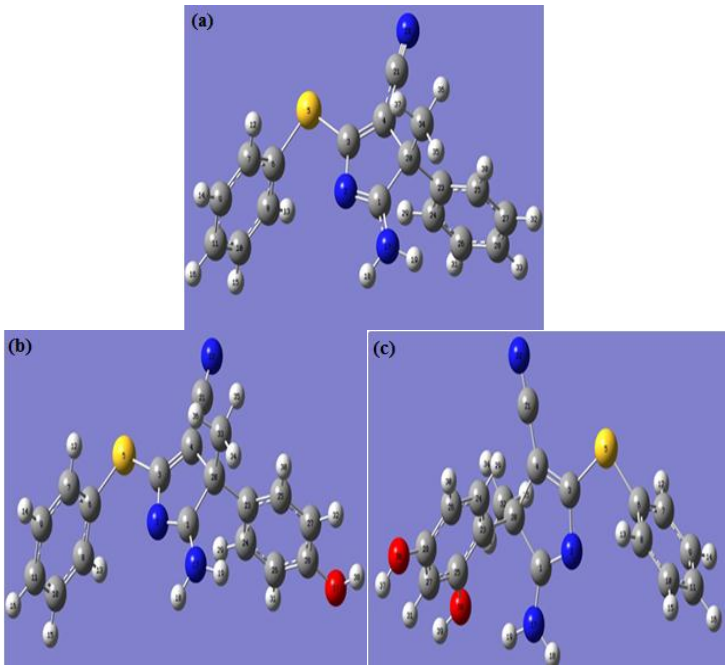

Fig. 6. Optimized structure of investigated inhibitors; (a) PPC-I, (b) PPC-II and (c) PPC-III

Table 8 represents the distribution of Mulliken atomic charges on the molecules undertaken in the present study. The frontier electron density distribution of the investigated inhibitor molecules are shown in Fig. 7. The parameters derived from quantum chemical calculations are given in Table 9. Generally, a high value of E_{HOMO} suggests the strong tendency to donate electrons into the low energy empty molecular orbital of the acceptor inhibitor molecule, while E_{LUMO} generally associated with tendency to accept the electrons from the donor molecule during donor-acceptor interaction [25].

Table. 8. Mulliken charge distributions of investigated inhibitors (PPCs)

PPC-I			**PPC-II**			**PPC-III**		
No	Atom	Mullikan charge	**No**	Atom	Mullikan Charges	**No**	Atom	Mullikan Charges
1	C	-0.011318	**1**	C	0.009997	**1**	C	0.233579
2	N	-0.001254	**2**	N	0.017366	**2**	N	-0.066968
3	C	-0.857245	**3**	C	-0.935207	**3**	C	-0.38117
4	C	0.245173	**4**	C	0.291906	**4**	C	0.267181
5	S	0.431354	**5**	S	0.398996	**5**	S	0.397495
6	C	0.247196	**6**	C	0.289976	**6**	C	0.293838
7	C	-0.123078	**7**	C	-0.073545	**7**	C	0.253454
8	C	-0.215114	**8**	C	-0.277321	**8**	C	-0.132915
9	C	-0.128603	**9**	C	-0.163275	**9**	C	-0.099459
10	C	-0.174026	**10**	C	-0.14526	**10**	C	-0.17706
11	C	-0.073515	**11**	C	-0.081354	**11**	C	-0.089928
17	N	-0.436109	**17**	N	-0.440237	**17**	N	-0.542031
20	C	0.344362	**20**	C	0.630889	**20**	C	0.399232
21	C	-0.422208	**21**	C	-0.403504	**21**	C	-0.868768
22	N	-0.56797	**22**	N	-0.569874	**22**	N	-0.505118
23	C	0.093841	**23**	C	0.111297	**23**	C	1.724581
24	C	-0.198531	**24**	C	-0.740718	**24**	C	-0.983572
25	C	-0.163582	**25**	C	-0.693002	**25**	C	-0.289603
26	C	0.077594	**26**	C	0.746984	**26**	C	-0.123682
27	C	-0.237297	**27**	C	0.378428	**27**	C	0.240326
28	C	-0.023425	**28**	C	-0.249243	**28**	C	-0.474815
34	C	-0.245908	**33**	C	-0.248773	**32**	C	-0.416591
			37	O	-0.513883	**36**	O	-0.521062
						38	O	-0.571477

From the results reported in Table 9, it can be concluded from the values of E_{HOMO} and E_{LUMO} that the values of inhibition efficiency of investigated inhibitors will be: PPC-III > PPC-II > PPC-I. Chemical hardness (η), softness (σ) and ΔE are other closely related quantum chemical calculations indices. The literature survey reveals that a molecule with high value of chemical hardness generally associated with low chemical reactivity which is responsible therefore low inhibition efficiency [25].

The molecule with high value of softness associated with high chemical polarization or deformation resulting in the high molecular volume and adsorption efficiency. The soft molecule consisted with low value of ΔE (E_{HOMO}-E_{LUMO}). According to our theoretical results, we can conclude the corrosion inhibition efficiency order as: PPC-III > PPC-II > PPC-I which is in good agreement to the experimental order of inhibition efficiency

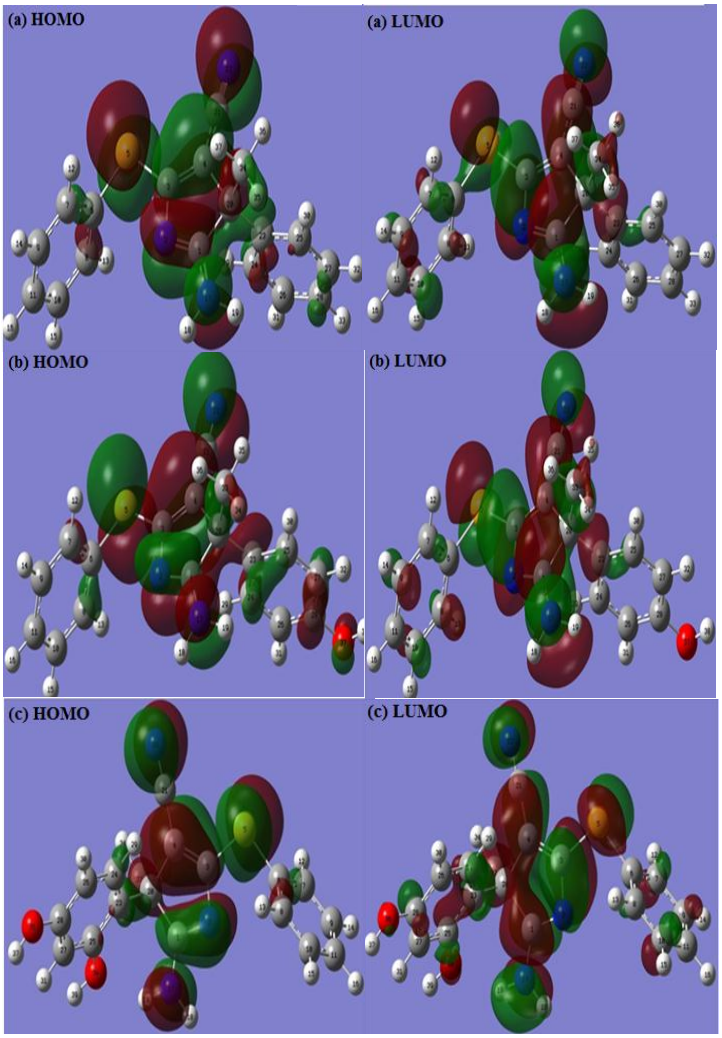

Fig. 7. The frontier molecular orbital density distribution of three PPCs (a) PPC-1 (left, HOMO; right, LUMO), (b) PPC-2 (left, HOMO; right, LUMO) and (c) PPC-3 (left, HOMO; right, LUMO)

Since the adsorption of inhibitors on the metal surface involve charge transfer processes, the concept of electronegativity is important during metal-inhibitor interaction [25,26]. From equation 6 it can be derived that the fraction of electron transfer between metal and inhibitor decreases as the electronegativity of inhibitor increases. In our present study the values of electronegativities of studied inhibitors follow the order: PPC-III < PPC-II < PPC-I which is just converse to the order of inhibition efficiency. Molecular electrostatic potential (MEP)

which describes the distribution of charge in the inhibitor molecule can also provide some insight into their adsorption behavior on the metallic surface and is a very useful descriptor for determining electrophilic attack and nucleophilic reaction as well as hydrogen bonding [27].

In our present study, the prediction of sites for electrophilic attack and nucleophilic reactions for investigated inhibitors has been carried out by MEP. Fig. 8 represents the MEP map of the studied PPCs. In the figure, red regions of MEP represent the sites for electrophilic attack whereas blue regions of MEP represent the sites for nucleophilic reactions. It can be seen from the Fig. 8 that regions for electrophilic attack mostly localized around pyrrole ring of the PPC-1 which is attributed due to presence of-NH_2 and -CN polar functional groups in addition to the N and S atoms of pyrrole ring and thiophenol moieties.

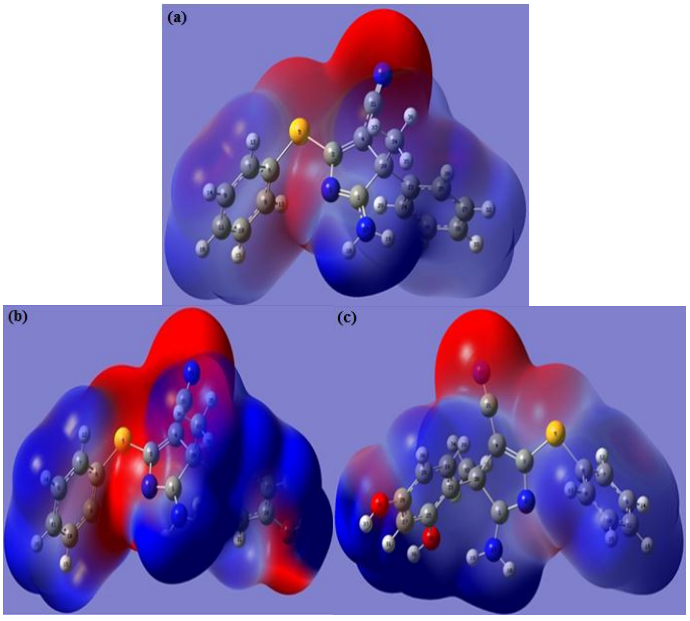

Fig. 8. Structure and electrostatic potential map for (a) PPC-I, (b) PPC-II and (c) PPC-III

Whoever, careful visualization of the Fig.8 shows that electrophilic regions were also localized over the aldehydic moiety along with pyrrole rings of the PPC-II and PPC-III. The localization of the red region over the aldehydic regions of PPC-II and PPC-III could be as a result of electron releasing ability of hydroxyl (-OH) group (s) of aldehydic moiety in the PPC-II and PPC-III [27,28].

Further, the blue regions which represent sites for nucleophilic reactions localized mostly over thiophenol and aldehyde rings for all studied inhibitors. This finding suggests that sites for electrophilic attacks (donation) mostly located around pyrrole ring while sites for nucleophilic reactions (retro donation) located over thiophenol and aldehydic moiety of the investigated inhibitors.

Table 9. Quantum chemical calculations parameters for investigated inhibitors (PPCs)

Quantum chemical Properties	**PPC-I** ($C_{18}H_{15}N_3S$)	**PPC-II** ($C_{18}H_{15}N_3OS$)	**PPC-III** ($C_{18}H_{15}N_3O_2S$)
Total energy (au)	-1257.42	-1332.64	-1407.8
E_{HOMO} (eV)	-0.21466	-0.21265	-0.2077
E_{LUMO} (eV)	-0.05703	-0.05578	-0.0508
ΔE (eV)	0.15763	0.15687	0.1566
Dipole moment (μ)	7.80262	7.96611	9.8228
Molecular Weight (amu)	305.399	321.398	337.39
Ionization potential (I) (eV)	0.21466	0.21265	0.2077
Electron affinity (A) (eV)	0.05703	0.05578	0.0508
Electronegativity (χ)	0.13584	0.13421	0.1292
Hardness (η)	0.07881	0.07843	0.07841
Softness (σ)	12.6879	12.746	12.7494
Fraction of electrons transferred (ΔN)	0.18499	0.18519	0.1857
Nucleophilicity (ω)	0.1064	0.11483	0.11707
ΔE_T	-0.0197	-0.0196	-0.019

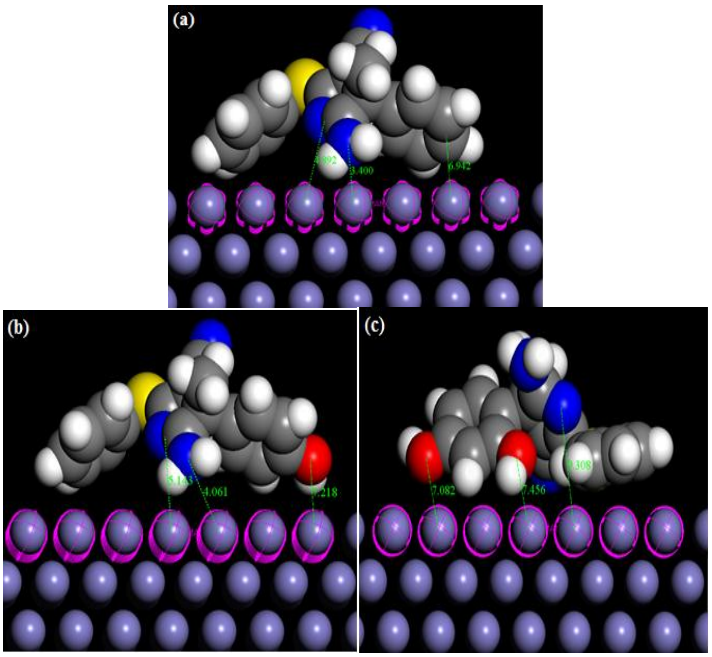

Fig. 9. Equilibrium configuration performed for PPCs on Fe (1 1 0) surface obtained by molecular dynamic simulations: (a) PPC-I, (b) PPC-II and (c) PPC-III

3.5. Molecular dynamics simulations studies

The molecular dynamics simulations were carried out to study the adsorption behavior of three PPCs molecules on the Fe (110) surface.

The molecular dynamics parameters was calculated when the temperature of the system containing Fe (110) surface and the inhibitors reaches to the equilibrium. Simulation results are shown in Fig. 9 and several molecular dynamics parameters are given in Table 10. It can be seen from the Fig. 9 that the PPCs molecules adsorbed on the Fe 9 (110) surface by nearly flat orientation via several polar functional groups such as –CN, -NH_2 and –OH in addition to the homo and hetero-aromatic rings. The large negative value of adsorption energy (Table 10) suggests that the inhibitor molecules can adsorb on Fe (110) surface strongly and spontaneously [29-31]. The value of adsorption energy follows the order: PPC-III > PPC-II > PPC-I which in accordance to the order of inhibition efficiency. The values of rigid adsorption energy also follow the same trend. The lowest energy of deformation energy for PPC-III among the studied compounds suggests that the PPC-III most easily deformed and polarized over metallic surface and cover maximum surface area and thereby exhibited maximum inhibition efficiency [32-35].

Table 10. Outputs and descriptors calculated by the Monte Carlo simulation for the lowest adsorption configurations of PPC-I, PPC-II and PPC-III Fe (110) surface (in kcal/mol)

Systems	E_{total}	E_{ads}	Rigid adsorption energy	Deformation energy	dE_{ad}/dN_i Inhibitors
Fe(110)/PPC-I	53.210	-4.006	-4.050	0.005	-4.006
Fe(110)/PPC-II	54.670	-4.155	-4.200	0.012	-4.155
Fe(110)/PPC-III	57.250	-5.147	-5.202	0.003	-5.147

4. CONCLUSIONS

In summary, 5-(phenylthio)-3H-pyrrole-4-carbonitriles (PPCs) act as good corrosion inhibitors and their efficiency increased in presence of electron releasing hydroxyl (-OH) groups. Adsorption of inhibitors obeyed the Langmuir adsorption isotherm. EIS study revealed that PPCs inhibit corrosion by adsorbing at metal/ acid solution interfaces. Polarization study revealed inhibitors acted as mixed type inhibitors Quantum chemical calculations and Molecular dynamics simulations studies supported the experimental results.

REFERENCES

[1] C. Verma, M. A. Quraishi, L. O. Olasunkanmi, and E. E. Ebenso, RSC Adv. 5 (2015) 85417.

[2] I. B. Obot, E. E. Ebenso, I. A. Akpan, Z. M. Gasem, and A. S. Afolabi, Int. J. Electrochem. Sci. 7 (2012) 1978.
[3] C. Verma, L. O. Olasunkanmi, E. E. Ebenso, M. A. Quraishi, and I. B. Obot, J. Phys. Chem. C 120 (2016) 11598.
[4] A. Rodger, R. Marrington, M. A. Geeves, M. Hicks, L. Alwis, D. J. Halsall, and T. R. Dafforn, Phys. Chem. Chem. Phys., 8 (2006) 3161.
[5] M. K. Awad, M. R. Mustafa, and M. M. A. Elnga, J. Mol. Struct. 959 (2010) 66.
[6] A. M. Fekry, and R. R. Mohamed, Electrochim. Acta. 55 (2010) 1933.
[7] N. Soltani, M. Behpour, E. E. Oguzie, M. Mahluji, and M. A. Ghasemzadeh, RSC Adv. 5 (2015) 11145.
[8] Y. Tang, X. Yang, W. Yang, Y. Chen, and R. Wan, Corros. Sci. 52 (2010) 242.
[9] P. Das, S. Ray, and C. Mukhopadhyay. J. Org. Lett. 15 (2015) 5622.
[10] C. Verma, E. E. Ebenso, I. Bahadur, I. B. Obot, and M. A. Quraishi, J. Mol. Liq. 212 (2015) 209.
[11] S. Karthikeyan, and P. A. Jeeva, Der. Pharm. Chem. 8 (2016) 118.
[12] M. J. Frisch, G .W. Trucks, H. B. Schlegel, G. E. Scuseria, and M. A. Robb, J. R. Cheeseman Jr. Gaussian 03, revision E.01.Wallingford, CT: Gaussian Inc (2007).
[13] P. Udhayakala, T. V. Rajendiran, S. Gunasekaran, and J. Comput. Meth. Mol. Des. 2 (2012) 1.
[14] A. M. Kumar, R. S. Babu, I. B. Obot, and Z. M. Gasem, RSC Adv. 5 (2015) 19264.
[15] C. Verma, M. A. Quraishia, and A. Singh, J. Taiwan Ins. Chem. Eng. 49 (2015) 229.
[16] N. Weder, R. A. Alberto, R. Koitz, J. Phys. Chem. C 120 (2016) 1770-1777.
[17] R. Solmaza, G. Kardas, M. C. ulhab, B. Yazıcı, and M. Erbil, Electrochimica Acta 53 (2008) 5941.
[18] K. M. Zohdy, Int. J. Electrochem. Sci. 10 (2015) 414.
[19] R. Mehdaoui, A. Khelifa, A. Khadraoui, O. Aaboubi, A. Hadj Ziane, F. Bentiss, and A. Zarrouk, Res. Chem. Intermed. 42 (2016) 5509.
[20] L. A. Nnanna, I. O. Owate, and E. E. Oguzie, Int. J. Mater. Eng. 4 (2014) 171.
[21] Y. Abboud , A. Abourriche , T. Ainane , M. Charrouf , A. Bennamara , O. Tanane, and B. Hammouti, Chem. Eng. Comm. 196 (2009) 788.
[22] C. Verma, and M. A. Quraishi, Ain Shams Eng. J. 7 (2016) 1.
[23] R. A. Bustamante, G. N. Silve, M. A. Quijano, H. H. Hernandez, M. R. Romo, A. Cuan, and M. P. Pardave, Electrochim. Acta 54 (2009) 5393.
[24] C. B. Verma, M. J. Reddy, and M. A. Quraishi, Anal. Bioanal. Electrochem. 6 (2014) 321.
[25] S. K. Saha, A. Dutta, P. Ghosh, D. Sukulc, and P. Banerjee, Phys. Chem. Chem. Phys. 17 (2015) 5679.
[26] R. Ferreira, Trans. Faraday Soc. 59 (1963) 1064.

[27] G. Gece, Corros. Sci. 50 (2008) 2981.
[28] H. Ma, S. Chen, B. Yin, S. Zhao, and X. Liu, Corros. Sci. 45 (2003) 867.
[29] M. Lebrini, M. Lagrenee, H. Vezin, M. Traisnel, and F. Bentiss, Corros. Sci. 49 (2007) 2254.
[30] Y. Tang, X. Yang, W. Yang, Y. Chen, and R. Wan, Corros. Sci. 52 (2010) 242.
[31] F. Zhang, Y. Tang, Z. Cao, W. Jing, Z. Wu, and Y. Chen, Corros. Sci. 61 (2012) 1.
[32] S. Xia, M. Qiu, L. Yu, F. Liu, and H. Zhao, Corros. Sci. 50 (2008) 2021.
[33] C. Verma, L. O. Olasunkanmi, I. B. Obot, E. E. Ebenso, and M. A. Quraishi, RSC Adv. 6 (2016) 53933.
[34] Y. Tang, X. Yang, W. Yang, R. Wan, Y. Chen, and X. Yin, Corros. Sci. 52 (2010) 1801.
[35] C. Verma, L. O. Olasunkanmi, I. B. Obot, E. E. Ebenso, and M. A. Quraishi, RSC Adv. 6 (2016) 15639.